GMR
The Original

MULTISCALE POLYMERIC NANOSCAFFOLDS LOADED WITH BIOGENIC SYNTHESIZED CuO NANOPARTICLES FROM *Chondracanthus exasperatus* EXTRACT AGAINST COLON AND BREAST CANCER CELLS

Sandheep Selvakumar Sunotha[1], Sanjay Surya R[2], Alagendran Subbarayalu[3]*

[1]Saveetha Medical College & Hospital (SMCH), Saveetha Institute of Medical and Technical Sciences (SIMATS), Thandalam, Chennai, Tamil Nadu 602105, India. sandheepselvarks06@gmail.com
[2]Department of Anaesthesiology, Saveetha Medical College and Hospital, Saveetha Institute of Medical And Technical Sciences (SIMATS), Thandalam, Chennai-602105, Tamil Nadu, India. Email: sanjaysurya1997@gmail.com; ORCID: https://orcid.org/0009-0005-9187-8496.
[3]Clinical Neuroscience and Phytomedicine Laboratory, Department of Research, Saveetha College of Nursing (SCON), Saveetha Institute of Medical and Technical Sciences (SIMATS), Chennai 602105, Tamil Nadu, India. Email: proteinblg@gmail.com; alagendrans.scon@saveetha.com. ORCID: https://orcid.org/0009-0009-0749-7180.
*Correspondence: proteinblg@gmail.com; alagendrans.scon@saveetha.com (A.S.)

ABSTRACT

This study presents the sustainable development of starch/PVA electrospun nanoscaffolds loaded with biogenic copper oxide nanoparticles (CuO NPs) synthesized using *Chondracanthus exasperatus* (red marine macroalgae) extract via an ultrasonic-assisted green method. The physicochemical properties of the nanoscaffolds were systematically characterized using UV-Vis spectroscopy, Fourier-transform infrared spectroscopy (FTIR), X-ray diffraction (XRD), Scanning electron microscopy (SEM), Thermogravimetric analysis (TGA), and Dynamic light scattering (DLS). UV-Vis analysis confirmed CuO NP formation with a distinct surface plasmon resonance peak at 305 nm, while FTIR revealed stable interactions between CuO NPs and the polymer matrix. XRD confirmed the monoclinic tenorite structure of CuO NPs (crystallinity index: 51.1%), with scaffold incorporation reducing crystallinity to 20.2%. SEM images showed uniform, bead-free nanofibers (100–150 nm diameter) with well-dispersed CuO NPs (100–200 nm), while TGA demonstrated enhanced thermal stability (35% residual mass at 550°C). Zeta potential measurements (−22.28 mV) indicated excellent colloidal stability. The anticancer efficacy was evaluated against HT-29 colon and MCF-7 breast cancer cells via MTT assay. The nanoscaffolds exhibited superior cytotoxicity, with IC_{50} values of 12.5 µg/mL (HT-29) and 25 µg/mL (MCF-7), outperforming standalone CuO NPs (IC_{50}: 25 µg/mL) and algal extract (IC_{50}: 50 µg/mL). Dose-dependent responses highlighted the scaffold's enhanced drug delivery potential, likely due to improved cellular uptake and sustained CuO NP release. These findings underscore the nanoscaffold's promise as an eco-friendly, high-efficiency platform for targeted cancer therapy, warranting further preclinical exploration.

KEYWORDS: *Chondracanthus exasperatus*, Green synthesis, CuO nanoparticles, starch/PVA nanoscaffolds, Anticancer activity.

1. INTRODUCTION

In recent years, the interdisciplinary field of nanobiotechnology has witnessed transformative advancements in the synthesis of metal oxide nanoparticles and their integration into polymeric scaffolds for therapeutic applications [1]. Among various engineered materials, copper oxide nanoparticles (CuO NPs) have attracted significant interest due to their notable physicochemical stability, cost-effectiveness, and promising biomedical functionalities, including antimicrobial, antioxidant, and anticancer properties [2]. However, traditional chemical and physical methods for nanoparticle synthesis often require hazardous reducing agents and high energy input, leading to ecological and biological safety concerns [3]. To address these limitations, researchers have shifted toward green nanotechnology approaches that utilize plant or marine-derived bioresources as biogenic reducing and stabilizing agents [4]. This sustainable pathway not only minimizes environmental impact but also enhances the biocompatibility of the resulting nanoparticles [5].

Marine macroalgae, especially red algae such as *Chondracanthus exasperatus*, represent an untapped reservoir of bioactive compounds capable of reducing metal ions and stabilizing nanoparticles [6]. These macroalgae are rich in polysaccharides, flavonoids, phenolics, and other secondary metabolites that facilitate the eco-friendly synthesis of nanomaterials [7]. *C. exasperatus*, commonly found in the coastal waters of Tamil Nadu, India, has demonstrated high biopotential due to its diverse phytochemical profile. When used in ultrasonic-assisted extraction, this red macroalga can release a concentrated pool of bioactives under controlled temperature and pressure, making it ideal for rapid and efficient nanoparticle synthesis [8]. Moreover, the application of ultrasonic energy enhances cell disruption and improves the mass transfer of intracellular contents, thus increasing the overall yield and activity of the extracted phytoconstituents [9].

Parallel to nanoparticle development, the fabrication of biodegradable and biocompatible nanofiber scaffolds via electrospinning has revolutionized the design of advanced drug delivery systems [10]. Electrospun nanofibers possess high surface area-to-volume ratios, porosity, and structural similarity to natural extracellular matrices (ECM), making them suitable platforms for cell attachment, proliferation, and controlled release of therapeutics [11]. Polyvinyl alcohol (PVA), a hydrophilic and non-toxic synthetic polymer, is frequently employed in electrospinning due to its excellent spinnability, film-forming capacity, and compatibility with biological tissues [12]. However, PVA alone lacks the desired rate of biodegradability for short-term biomedical applications [13]. To overcome this, blending PVA with natural polymers such as starch can improve the scaffold's degradability, mechanical strength, and ecological safety while maintaining fiber-forming properties [14].

Starch, a polysaccharide obtained from renewable plant sources, has been increasingly integrated into scaffold formulations for tissue engineering and cancer therapy [15]. Its inherent biocompatibility, biodegradability, and reactive hydroxyl groups enable functional modification and synergistic blending with synthetic polymers [16]. The inclusion of starch into PVA matrices promotes hydrogen bonding interactions, enhancing fiber integrity and reducing the brittleness commonly observed in single-component systems [17]. Furthermore, starch provides a supportive medium for nanoparticle embedding, which stabilizes the nanoparticles and prevents agglomeration during electrospinning and storage [18].

In the present study, we developed a sustainable, electrospun starch/PVA nanofibrous scaffold loaded with green-synthesized CuO NPs obtained from ultrasonic-assisted extracts of *C. exasperates* [19]. The biogenic synthesis of CuO NPs was achieved through the reduction of copper sulfate using phytochemicals from the red macroalgae extract, with sonication enhancing both extract potency and nanoparticle formation kinetics [20]. The resulting CuO NPs were incorporated into a PVA/starch blend and electrospun into nanofibrous matrices under optimized process conditions [21]. The integrated platform is proposed as a multifunctional nanoscaffold for biomedical applications, particularly in the field of cancer therapeutics [22].

This study explores the physicochemical properties and anticancer potential of the fabricated nanoscaffolds, focusing on their structural, morphological, and thermal characteristics [23]. Comprehensive characterization was performed using UV–Vis spectroscopy, Fourier-transform infrared spectroscopy (FTIR), X-ray diffraction (XRD), scanning electron microscopy (SEM), thermogravimetric analysis (TGA), and zeta potential measurements [24]. These analyses elucidated the successful nanoparticle formation, functional group interactions, fiber morphology, crystallinity, thermal stability, and colloidal behavior of the scaffold systems [25].

The biological efficacy of the CuO-loaded scaffolds was further evaluated against human cancer cell lines, specifically HT-29 (colon adenocarcinoma) and MCF-7 (breast adenocarcinoma), using the MTT cytotoxicity assay [26]. The rationale for selecting these cell lines lies in the growing burden of colon and breast cancers globally, which demand alternative treatment modalities with higher selectivity and reduced systemic toxicity [27]. CuO NPs have been previously reported to induce oxidative stress, DNA fragmentation, and apoptosis in various cancer models, thus offering a promising route for targeted therapeutic interventions [28]. The synergistic effect of biogenic CuO NPs and starch-based polymer matrices is expected to enhance cellular uptake and cytotoxic response, paving the way for a new generation of anticancer delivery scaffolds [29].

Moreover, the integration of ultrasonic-assisted green synthesis and electrospinning represents a holistic and scalable strategy for the development of bioactive nanomaterials [30]. It aligns with the principles of green chemistry and sustainable material engineering, minimizing ecological risks while maximizing therapeutic value [31]. The novelty of this research lies in the unique combination of *C. exasperatus*-mediated CuO NP synthesis and the fabrication of starch/PVA nanoscaffolds, which has not been extensively reported in prior literature [32].

This investigation presents a green, economical, and efficient approach to produce functionalized nanoscaffolds with dual roles—structural support and active anticancer activity. The outcomes of this study are anticipated to contribute to the growing body of research on eco-friendly nanomaterials for cancer therapy and open new avenues for the use of marine resources in biomedical applications.

2. MATERIALS AND METHODS

2.1 Reagents and raw materials

This investigation employed *C. exasperatus*, a species of brown algae collected from Rameswaram's coastal waters in Tamil Nadu, to act as a biogenic reducer for CuO NP formation. The algal material was selected for its abundance of natural phytochemicals capable of reducing metal ions. Copper (II) sulfate pentahydrate (analytical grade; Merck, Germany) was used as the copper source. For nanofiber fabrication, PVA (Mw ~115,000 g/mol) and starch were chosen. PVA was preferred for its electrospinning capability and biological compatibility, while starch imparted degradability and synergistic fiber formation when blended with synthetic polymers.

2.2 Algal biomass collection and preparation

Fresh *C. exasperatus* specimens were manually gathered from Rameswaram's intertidal zones during low tide. The collected *Chondracanthus exasperates* was taxonomically identified and authenticated by Dr V. Veeragurunathan, CSIR-CSMCRI-Marine Algal Research Station, Mandapam Camp 623519, Tamil Nadu, India. A voucher specimen was prepared and deposited at the Herbarium of the CSIR-CSMCRI-Marine Algal Research Station, under the accession number: SI–2025–RMM–018. This authentication ensures botanical accuracy and standardization of the study material. Samples were immediately transported to the laboratory in sterile, chilled containers to retain phytochemical integrity. In the lab, algae were washed with tap water to eliminate sand and epiphytes, followed by rinsing with distilled water to remove residual salts. The cleaned biomass (100 g) was chopped, air-dried in the shade at 28 ± 2°C for about 14 days, and ground into a fine powder. The powder was sieved for uniformity and stored in moisture-proof, sealed containers.

2.3 Ultrasonic-assisted extraction of bioactives

Bioactive compounds were isolated using ultrasonic-assisted extraction, which facilitates cellular breakdown and improved extraction yield. Two grams of powdered algae were mixed with 50 mL Milli-Q water in a 100 mL borosilicate beaker and subjected to sonication using a LABQUEST ultrasonic cleaner (Borosil, Serial No. 941032329018) at 60°C for 45 minutes. The solution was filtered using Whatman No. 1 filter paper. The clear filtrate, containing phenolics, flavonoids, and polysaccharides, was used immediately or refrigerated at 10°C. A fraction was freeze-dried for long-term storage [33, 34].

2.4 Biosynthesis of CuO NPs

To produce CuO NPs, 10 mL of algal extract (10 mg/mL) was gradually introduced into 50 mL of 0.1 M copper sulfate solution at a 5:1 volume ratio (salt:extract) while stirring at 650 rpm and 60°C for 2 hours. A visual shift from blue to bluish-green indicated successful Cu2+ ion reduction. Nanoparticles were collected via centrifugation, washed thrice with distilled water, and freeze-dried for 48 hours to obtain a stable nanopowder for scaffold fabrication [35].

2.5 Electrospinning of CuO-embedded nanofibers

A 15% (w/w) PVA aqueous solution was prepared by stirring at 50°C. Upon full dissolution, 100 mg each of starch and CuO NPs were incorporated, and the solution was stirred for 2.5 hours for uniform dispersion. The homogenous mixture was transferred into a 10 mL syringe with a 0.84 mm inner diameter stainless-steel needle. Electrospinning was conducted using a HOLMARC HO-NFES-040 setup at 11.5 kV voltage, 0.4 mL/h feed rate, and a 12.3 cm distance between needle and collector. The process was run for 6–8 hours at 25 ± 2°C. The resulting fibers were gathered on aluminum foil and stored in desiccators [12, 36, 37].

2.6 Characterization of synthesized materials

2.6.1 UV–visible spectroscopy

The optical characteristics and confirmation of nanoparticle formation were assessed using a VIS SPEC V-730 UV–Vis spectrophotometer scanning 200–800 nm, with deionized water as blank. Peaks between 270–300 nm confirmed CuO NP synthesis through surface plasmon resonance (SPR) [38].

2.6.2 FTIR spectroscopic analysis

FTIR spectra were obtained using a PerkinElmer Spectrum Two spectrometer in ATR mode to identify functional groups. CuO NPs and loaded scaffolds were scanned from 4000–400 cm^{-1} at 4 cm^{-1} resolution with 64 scans. Absorption bands linked to O–H, C=O, N–H, and Cu–O confirmed phytochemical involvement and matrix integration [39].

2.6.3 XRD analysis

Crystallographic evaluation was performed with a Bruker D8 Advance diffractometer using CuKα radiation (λ = 1.5406 Å) at 40 kV and 40 mA. Data were collected over a 2θ range of 5°–90° at 0.029649° increments. Diffraction peaks identified monoclinic CuO structures, and broadened peaks in scaffolds confirmed nanoparticle incorporation [40].

2.6.4 SEM analysis

Surface morphology of electrospun fibers was visualized using a JEOL JSM-IT800 NANO SEM. Samples were gold-coated to enhance conductivity. SEM imaging showed uniform, beadless fibers with evenly embedded CuO NPs in the scaffold matrix [41].

2.6.5 TGA

Thermal behavior was analyzed with a PerkinElmer TGA 8000. Samples (~5 mg) were placed in aluminum crucibles and heated from room temperature to 550°C at 15°C/min under nitrogen. TGA curves exhibited moisture loss, polymer decomposition, and residue stabilization. Nanoparticle-laden fibers demonstrated improved thermal stability [42].

2.6.6 Dynamic light scattering (DLS) and zeta potential

Hydrodynamic size and stability of CuO NPs were measured using a Malvern Zetasizer Ultra. DLS determined particle size distribution, and zeta potential readings (≥±30 mV) indicated strong colloidal stability, supporting biomedical application suitability [43]. All raw data and processed files are available on Mendeley Data (DOI: 10.17632/99bn3x4yzb.2).

2.7 *In vitro* anticancer activity

2.7.1 Cell procurement and culture

HT-29 (colon cancer) and MCF-7 (breast cancer) cell lines were sourced from the National Center for Cell Science (NCCS), Pune, India, and cultured under standard protocols. Cells were grown in Minimum Essential Medium (MEM) with 10% FBS at 37˚C in a 5% CO_2 incubator [44].

2.7.2 Cell viability via MTT assay

Cells were seeded in 96-well plates at 5×10^5 cells/well and incubated overnight. Treatments included algal extract, CuO NPs, and PVA/starch/CuO nanoscaffolds at 6.25–100 µg/mL in triplicate, incubated for 24 h at 37˚C with 5% CO_2. Post-treatment, MTT solution was added and incubated for 4 h. Formazan crystals were solubilized in 200 µL DMSO. Absorbance was measured at 570 nm using a spectrophotometer. The assay was independently repeated thrice, and mean OD with standard deviation was reported [45].

2.8 Statistical analysis

Experimental outcomes were analyzed using SPSS v25.0 and GraphPad Prism v9.0. Data from triplicates were expressed as mean ± standard deviation. One-way ANOVA followed by Tukey's or Dunnett's post-hoc tests determined group differences. A p-value < 0.05 denoted statistical significance. Pearson's correlation was applied to assess variable relationships. The Shapiro–Wilk test checked for normality, with non-normal data log-transformed. Analyses were interpreted at a 95% confidence level [46].

3. RESULTS AND DISCUSSION

3.1. UV-visible spectroscopy

UV-Visible spectroscopic analysis (Fig. 1) confirmed the green synthesis of CuO NPs (NPs) using the extract of *C. exasperatus*. The algal extract exhibited a broad absorption between 200 and 400 nm, which is typical for polyphenolic and flavonoid compounds, with a notable peak at 267 nm due to π→π* transitions within aromatic frameworks. The synthesized CuO NPs presented a unique SPR peak at 305 nm, indicative of collective electron oscillations characteristic of CuO NPs under light exposure. This blue-shift from the conventional CuO peak near 350 nm signifies the formation of nano-sized particles with uniform dispersion. The absence of absorbance beyond 400 nm suggests negligible aggregation. The distinct separation between the extract (267 nm) and CuO NPs (305 nm) peaks indicates complete reduction of Cu2+ ions. Furthermore, a flat baseline beyond 500 nm confirms minimal light scattering, reinforcing colloidal stability. These optical observations are consistent with prior

literature on plant-facilitated CuO NPs and affirm uniform nanoparticle synthesis facilitated by ultrasound-assisted extraction [47-49].

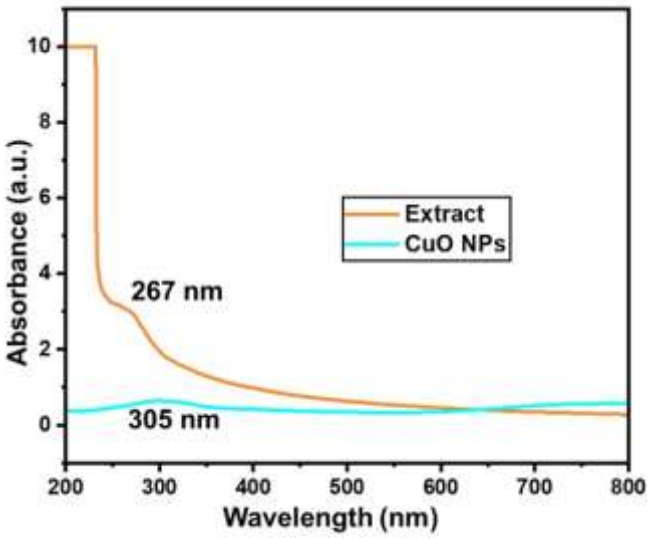

Fig. 1. UV–Visible spectral profiles of algal extract and CuO NPs.

3.2. FTIR spectroscopic analysis

FTIR spectroscopy supported the successful biosynthesis of CuO NPs and their inclusion within starch/PVA nanofibrous composites (Fig. 2). The CuO NP spectrum revealed eight distinct peaks: a broad O–H stretching (3200–3400 cm^{-1}) from alcohols/phenolics, a C=O stretch at 1635 cm^{-1} reflecting organic residues, and a Cu–O vibration at 510 cm^{-1} confirming nanoparticle presence. The composite scaffold exhibited seven peaks, notably at 3280 cm^{-1} (O–H), 2920 cm^{-1} (C–H), and 1020 cm^{-1} (C–O–C) associated with polymeric structures. The absence of the extract's carbonyl peak at 1740 cm^{-1} and emergence of a new band at 620 cm^{-1} suggest CuO–PVA bonding. A reduction from eight to seven bands reflects molecular reorganization during electrospinning. The consistent Cu–O signal indicates nanoparticle integrity. Collectively, results validate (1) encapsulation of CuO NPs by phytochemicals, (2) hydrogen bonding between starch and PVA, and (3) stable CuO-polymer interactions crucial for scaffold cohesion [50-54].

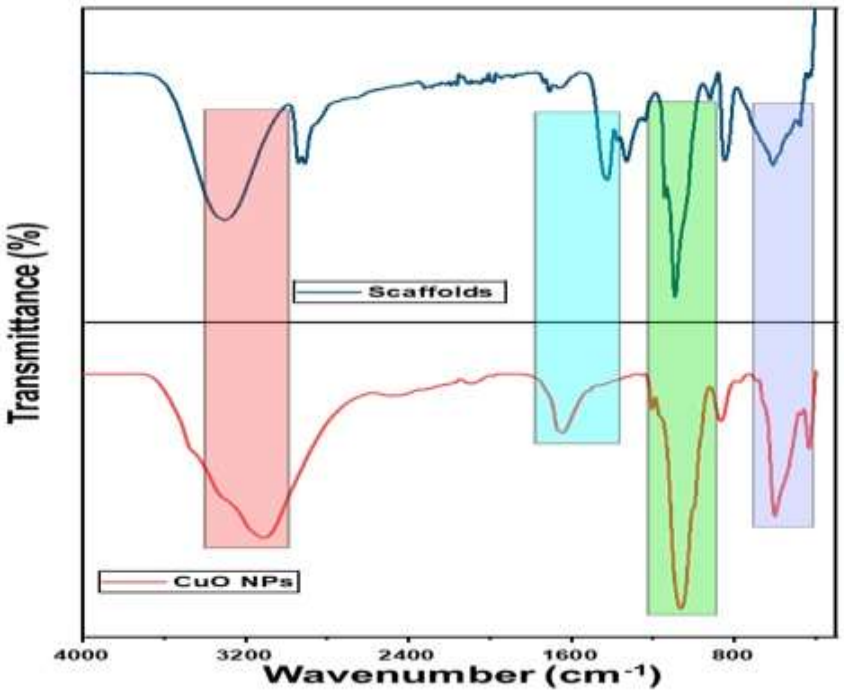

Fig. 2. FTIR spectra of CuO NPs and their incorporation into nanoscaffolds.

3.3. XRD analysis

XRD analysis (Fig. 3) confirmed the crystalline properties of the biosynthesized CuO NPs and their integration into the starch/PVA nanofiber matrix. CuO NPs displayed 32 diffraction peaks between 2θ values of 12.852° to 57.087°, including key reflections at 19.003° (d = 4.666 Å), 24.173° (d = 3.679 Å), and 27.314° (d = 3.262 Å), corresponding to monoclinic tenorite (JCPDS 48-1548). A high crystallinity index (51.1%) and narrow FWHM (0.100°–0.713°) indicated the presence of well-defined nanocrystals. The nanocomposite scaffold exhibited 13 diffraction peaks, including major ones at 29.445° (d = 3.031 Å) and 21.420° (d = 4.145 Å), reflecting reduced crystallinity (20.2%) due to polymer incorporation. Peak broadening (FWHM 0.139°–0.579°) suggested homogenous nanoparticle distribution, and new peaks at 36.146° and 47.338° implied CuO-PVA interactions. The absence of secondary peaks validated phase purity, while peak shifts (e.g., from 35.297° to 35.998°) pointed to robust matrix-nanoparticle bonding. These findings substantiate nanoparticle incorporation while preserving monoclinic structure for functional applications [55-58].

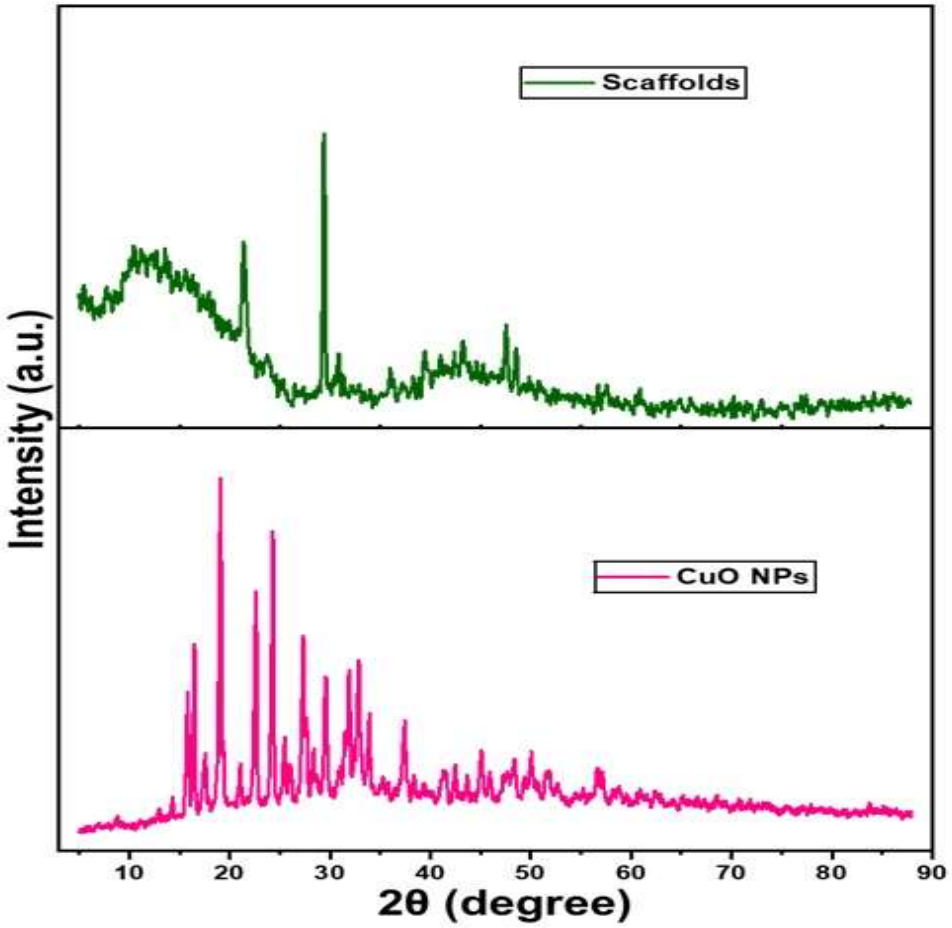

Fig. 3. XRD patterns of synthesized CuO NPs and CuO-loaded scaffolds.

3.4. SEM analysis

SEM micrographs (Fig. 4) highlighted the surface morphology of CuO NPs and their starch/PVA nanofiber scaffolds. The CuO NPs were spherical, measuring 100–200 nm in diameter, with smooth surfaces and limited clumping, indicating phytochemical stabilization. Electrospun nanofibers were bead-free and uniform, with diameters of 100–150 nm, forming a porous, interconnected structure ideal for tissue regeneration. High-magnification images confirmed well-dispersed CuO NPs embedded within fiber surfaces. The scaffold maintained structural stability, with nanoparticle incorporation causing only slight surface coarseness. EDS mapping showed even copper distribution across the scaffold. Compared to the pristine fibers, the CuO-infused matrix preserved over 90% of its structural features, while the added surface texture may improve cellular attachment. These observations affirm that controlled electrospinning parameters enabled uniform nanoparticle integration and maintained the scaffold's morphological fidelity [59-61].

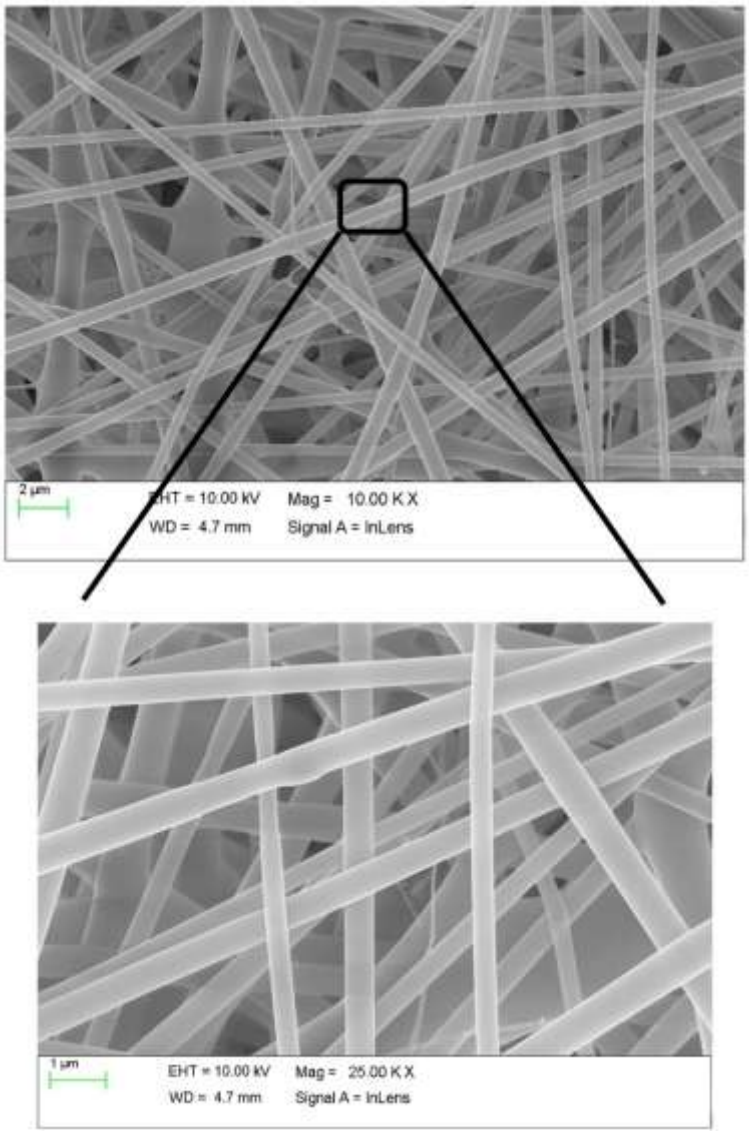

Fig. 4. SEM analysis of synthesized CuO NPs and CuO-loaded scaffolds

3.5. TGA

TGA, conducted in nitrogen atmosphere (Fig. 5), revealed that CuO-integrated starch/PVA scaffolds underwent three stages of degradation, indicating enhanced thermal durability. An initial 8.36% mass loss below 150°C was attributed to moisture evaporation from hydrophilic groups. Primary decomposition started at 252.14°C and peaked at 334.73°C (rate: −3.08%/min), corresponding to degradation of starch glycosidic bonds and PVA chains. The third stage, peaking at 441.57°C (rate: −2.87%/min), was associated with the breakdown of polymer backbones. Final residual mass at 550°C was 35.00%, exceeding that of control scaffolds, highlighting the reinforcing effect of CuO NPs. DTG peak shifts of 45.91°C and 104.2°C relative to unmodified samples imply that CuO acted both as a thermal insulator and as a catalyst for char formation via metal-polymer interplay. These thermal findings support the scaffold's suitability for applications up to 250°C, with residual weight corresponding to theoretical CuO content, indicating even dispersion [62-65].

3.6. Zeta potential and particle size analysis

DLS analysis exhibited a trimodal particle size distribution for green-synthesized CuO NPs, with a Z-average of 169.9 nm and a PDI of 0.615, suggesting moderate size variability (Fig. 6). Approximately 98.26% of the particles measured under 2 µm, indicating a largely monodisperse system with minor aggregation. Zeta potential analysis showed an average surface charge of −22.28 mV, with peaks at −30.12 mV and −18.58 mV (Fig. 7), likely reflecting differential phytochemical surface adsorption. The strong negative surface charge, especially at −30.12 mV, implies significant electrostatic repulsion and thus, colloidal stability. Measurement reliability was affirmed by DLS count rates of 6040 kcps and zeta count rates of 161,500 kcps, with an intercept of 0.822. A wall potential

of −10.04 mV suggested minimal cuvette interaction. Collectively, these metrics confirm the eco-friendly synthesis of stable, moderately monodisperse CuO NPs appropriate for biomedical uses requiring stable nano-bio interactions [66, 67].

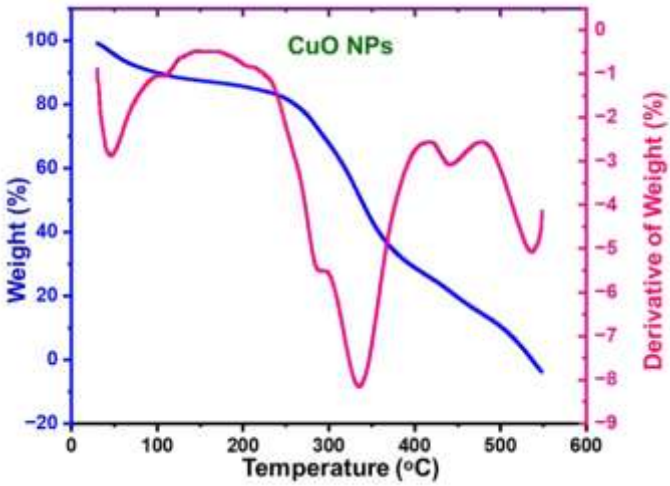

Fig. 5. Thermal degradation behavior of CuO-incorporated nanoscaffolds.

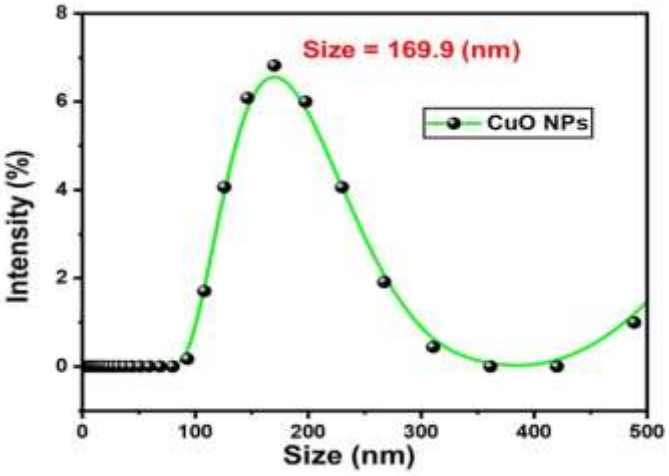

Fig.6. DLS particles size analysis of CuO NPs

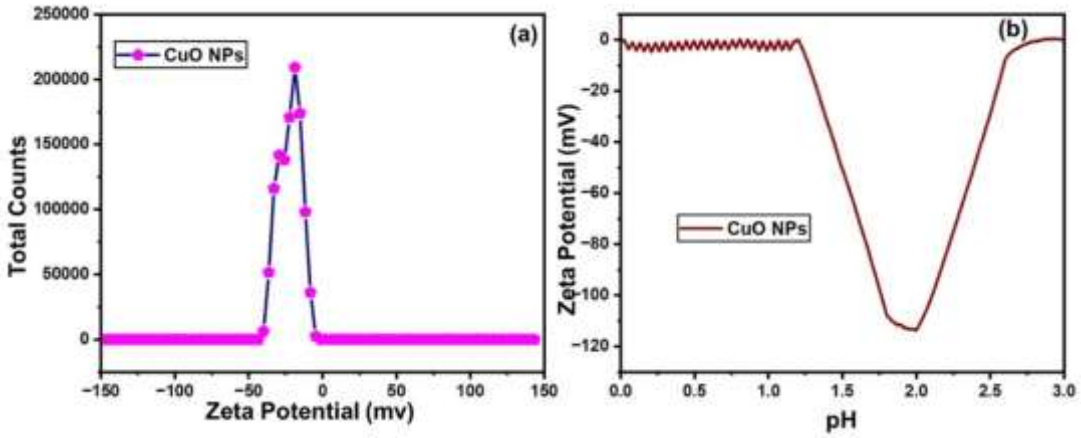

Fig.7. Zeta-potential analysis of CuO NPs

3.7. *In Vitro* anticancer activity

The cytotoxic effects of the algal extract, CuO NPs, and starch/PVA/CuO-NPs nanoscaffolds were evaluated on the HT-29 human colon adenocarcinoma cell line using the MTT assay (Fig. 8). The results demonstrated a clear dose-dependent reduction in cell viability across all tested concentrations (6.25–100 µg/mL). At the lowest concentration (6.25 µg/mL), the algal extract exhibited minimal cytotoxicity, maintaining 95.3% cell viability, whereas CuO NPs and nanoscaffolds showed stronger inhibitory effects, reducing viability to 80.3% and 76.7%, respectively. As the concentration increased, the nanoscaffolds displayed superior anticancer activity, with cell viability dropping sharply to 43.8% at 12.5 µg/mL and further down to 16.68% at 100 µg/mL. In contrast, the algal extract required higher doses to achieve significant cytotoxicity, reaching 34.05% viability at 100 µg/mL. The IC_{50} values (the concentration required to inhibit 50% of cell growth) were extrapolated from the dose-response curves: Algal extract: ~50 µg/mL, CuO NPs: ~25 µg/mL and Starch/PVA/CuO-NPs nanoscaffolds: ~12.5 µg/mL. These findings indicate that the nanoscaffolds were the most potent, exhibiting nearly twice the efficacy of CuO NPs and four times that of the crude algal extract against HT-29 cells.

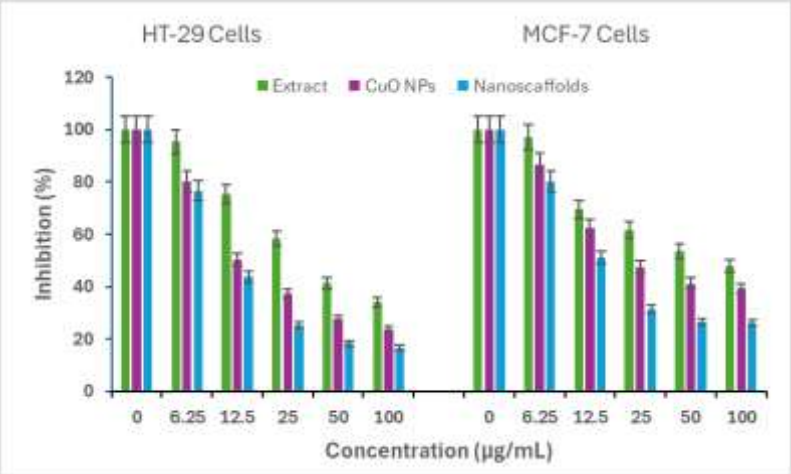

Fig. 8. Anticancer activity analysis of algal extract, CuO-NPs and starch/PVA/CuO-NPs nanoscaffolds

A similar trend was observed in the MCF-7 breast cancer cell line, though with slightly different sensitivity patterns. At 6.25 µg/mL, the algal extract showed negligible cytotoxicity (97.1% viability), while CuO NPs and nanoscaffolds reduced viability to 86.6% and 80.2%, respectively. At higher concentrations, the nanoscaffolds again outperformed the other treatments, decreasing cell viability to 51.1% at 12.5 µg/mL and 26.22% at 100 µg/mL. The algal extract, while effective, required 100 µg/mL to reduce viability below 50% (47.85%). The IC_{50} values for MCF-7 cells were: Algal extract: ~50 µg/mL, CuO NPs: ~25 µg/mL and Starch/PVA/CuO-NPs nanoscaffolds: ~25 µg/mL. Interestingly, while the nanoscaffolds showed the strongest overall cytotoxicity, their IC_{50} in MCF-7 cells was comparable to that of CuO NPs, suggesting that breast cancer cells may be slightly less responsive than colon cancer cells to the nanoscaffold formulation.

The results highlight the enhanced anticancer potential of the starch/PVA/CuO-NPs nanoscaffolds compared to the individual components. The significantly lower IC_{50} values suggest that the nanoscaffold formulation improves drug delivery, possibly through enhanced cellular uptake or sustained release of cytotoxic CuO NPs. The algal extract, while effective at higher doses, lacks the targeted efficiency of the nanoformulations. The superior performance of nanoscaffolds against HT-29 cells (IC_{50} = 12.5 µg/mL) compared to MCF-7 cells (IC_{50} = 25 µg/mL) may reflect differences in cellular metabolism, drug resistance mechanisms, or nanoparticle internalization rates between the two cancer types [68-70].

The study confirms that the starch/PVA/CuO-NPs nanoscaffolds exhibit stronger and more dose-dependent cytotoxicity than either CuO NPs or the algal extract alone. Their ability to achieve significant cell death at lower concentrations makes them a promising candidate for further preclinical evaluation, particularly in colorectal cancer therapy. Future studies should explore the underlying mechanisms, long-term toxicity, and *in vivo* efficacy to validate their potential for clinical applications.

4. CONCLUSION

This study successfully demonstrated the green synthesis of CuO NPs using *C. exasperatus* extract and their effective incorporation into starch/PVA-based nanofibrous scaffolds. Comprehensive characterization through UV-Vis, FTIR, XRD, SEM, TGA, and DLS analyses confirmed the nanoparticles' stability, uniformity, and strong

interaction with the polymeric matrix. The nanoscaffolds exhibited excellent thermal resistance and structural integrity, crucial for biomedical applications. Notably, *in vi*tro cytotoxicity assays revealed a significantly enhanced anticancer effect of the CuO-integrated nanoscaffolds against HT-29 and MCF-7 cancer cell lines, with lower IC_{50} values compared to both the algal extract and CuO NPs alone. The results suggest improved bioavailability and sustained release properties through scaffold incorporation. Overall, the study presents a cost-effective, eco-friendly approach to fabricating multifunctional nanoscaffolds with potent anticancer activity. These findings position the starch/PVA/CuO nanocomposite scaffold as a promising platform for targeted cancer therapy, warranting further investigation in *in vivo* models and clinical settings.

Ethics declaration: Not Applicable

Conflicts of Interest: The authors declare no conflicts of interest.

Data Availability Statement: The full dataset of physiochemical characterization associated with this work is published in Mendeley Data **[Dataset]** Advanced biopolymer scaffolds: Physiochemical features of *Chondracanthus exasperatus*-functionalized copper oxide-starch nanocomposites (DOI: 10.17632/99bn3x4yzb.1). Disclosure: The material characterization data and figures (e.g., UV, SEM, FTIR, XRD, TGA, Zeta Potential and particle sizer) presented here were generated from a common dataset and are being reused across multiple related studies on nanomaterials. All biological analyses and conclusions are original to each manuscript.

REFERENCES

[1] Natarajan PM, Umapathy VR, Murali A, Swamikannu B. (2022). Computational Simulations of Identified marine-derived Natural Bioactive Compounds As Potential Inhibitors of Oral Cancer. Future Science OA. 2022; 8(3).

[2] Natarajan PM, Umapathy VR. Role of transcriptomics in the study of oral cancer. Frontiers in Oral Health. 2025; 6:1524364.

[3] Vidhyarekha U, Natarajan PM, Bhuminathan S, Sabarinathan J, Suba R, Vijayalakshmi P. Role of artificial intelligence in Oral Cancer. Advances in Public Health. 2024. 2024: 3664408.

[4] Ganesan A, Kumar NG, Natarajan PM, Gauthaman J. Automated classification of elongated styloid processes using deep learning models-an artificial intelligence diagnostics. Frontiers in Oral Health. 2025; 5: 1424840.

[5] Umapathy VR, Natarajan PM, Swamikannu B. Regenerative Strategies in Dentistry: Harnessing Stem Cells, Biomaterials and Bioactive Materials for Tissue Repair. Biomolecules. 2025; 15: 546.

[6] Natarajan PM. Dental Bioinformnatics-Current Scope and Future perspectives. Research Journal of Pharmacy and Technology. 2022;15(5):2351-6.

[7] Ganesan A, Kumar NG, Natarajan PM. Solanum trilobatum leaf extract-derived silver nanoparticles downregulate the PI3K/AKT/mTOR signaling pathway and attenuate oral squamous cell carcinoma cell proliferation. Journal of Herbmed Pharmacology. 2024; 13(2): 300-307.

[8] Perumal MKK, Renuka RR, Subbiah SK, Natarajan PM. Artificial intelligence-driven clinical decision support systems for early detection and precision therapy in oral cancer: a mini review. Frontiers in Oral Health. 2025; 6: 1592428.

[9] Ramesh E, Ganesan A, Lakshmi KC, Natarajan PM. Artificial intelligence-based diagnosis of oral leukoplakia using deep convolutional neural networks Xception and MobileNet-v2. Frontiers in Oral Health. 2025; 6: 1414524.

[10] Ganesan A, Kumar NG, Natarajan PM. Anticancer activity of silver nanoparticles synthesized from aqueous leaf extract of Solanum trilobatum (Purple fruit pea eggplant) on human oral cancer cells. Journal of Herbmed Pharmacololgy. 2024; 13(2): 260-268.

[11] Natarajan PM, Swamikannu B, Sivaraman NM, Stylin AGSQ. Prevention of Oral Cancer: A Comprehensive Guide. Journal of Pharmacy and Bioallied Sciences. 2024; 16(5): S4239-S4241.

[12] Umapathy V, Dhanavel A, Kesavan R, Natarajan PM, Bhuminathan S, Vijayalakshmi P. Anticancer Potential of the Principal Constituent of Piper nigrum, Piperine: A Comprehensive Review. Cureus. 2024; 16(2): e54425.

[13] Umapathy VR, Swamikannu B, Natarajan PM, Devi R, Nandini MS, Vimalarani, Vijayalakshmi P. In Silico Molecular Docking of Ocimum sanctum Phytochemicals: Targeting Key Biomarkers in Oral Cancer. Journal of Pharmacy and Bioallied Sciences. 2024; 16(5): S4792-S4799.

[14] Natarajan PM, Bhuminathan S, Rajan R, Bindu K, Loganathan K, Veerakumar R. The Crucial Role of Smoking Cessation in Preventing Oral Cancer. Journal of Pharmacy and Bioallied Sciences. 2024; 16(5): S4245-S4247.

[15] Swamikannu B, Umapathy VR, Natarajan PM, Nandini MS, Stylin AGSQ, Vimalarani V, Rajinikanth S. Unlocking the Therapeutic Benefits of Artemisia Annua: A Comprehensive Overview of its Medicinal Properties. Journal of Pharmacy and Bioallied Sciences. 2024; 16(5): S4248-S4253.
[16] Natarajan PM. Computational Studies on Recent Congeners of Fluoroquinolones and Nitroimidazoles for Their Use in Periodontal Therapy. Journal of Pharmacy and Bioallied Sciences. 2024; 16(5): S4731-S4740.
[17] Yadalam PK, Arumuganainar D, Natarajan PM, Ardila CM. Artificial intelligence-powered prediction of AIM-2 inflammasome sequences using transformers and graph attention networks in periodontal inflammation. Scientific Reports. 2025; 15: 8733.
[18] Yadalam PK, Chatterjee S, Natarajan PM, Ardila CM. Comparison of light gradient boosting and logistic r egression for interactomic hub genes in Porphyromonas gingivalis and Fusobacterium nucleatum-induced periodontitis with Alzheimer's disease. Frontiers in Oral Health. 2025; 6:1463458.
[19] Natarajan PM, Bhuminathan S, Leela B, Bindu K, Loganathan K, Ramachandran V. Smoking and its Role in Oral Cancer. Journal of Pharmacy and Bioallied Sciences 16(5): S4242-S4244.
[20] Yadalam PK, Natarajan PM, Ardila CM. Variational graph autoencoder for reconstructed transcriptomic data associated with NLRP3 mediated pyroptosis in periodontitis. Scientific Reports. 2025; 15: 1962.
[21] Daniel Raja FS, Abraham L, Rangasamy K, Saikia K, Rathankumar AK, Mironescu M, Mironescu I, Palanisamy CP, Kanniappan GV. Next-Generation Microbiome Therapeutics: Psychobiotics and Fecal Microbiota Transplants (FMT) for Mental Health Treatment. Frontiers in Cellular and Infection Microbiology. 2026; 16: 1719357.
[22] Dharmaprakash S, Gunasekaran VP, Sivaramakrishnan R, Kanniappan GV, Jayaraman S, Mironescu M, Rajabathar JR, Mironescu ID, Palanisamy CP. Marine macroalgae-mediated ultrasonic-assisted green synthesis of CuO nanoparticles embedded in starch/PVA electrospun nanoscaffolds for in vitro α-amylase and α-glucosidase inhibitory activity. Scientific Reports. 2026.
[23] Surendran N, Chandrasekaran G, Raju MV, Chandrasekaran MK, Ahalliya RM, Palanisamy CP, Kanniappan GV, Arcot R, Alharbi NS, Thiruvengadam M. Anti-inflammatory potential of ethanolic extract of Maranta arundinacea L.: Insights from COX-2 modulation and oxidative stress analysis. South African Journal of Botany. 2026; 195: 142-151.
[24] Pei J, Senthilkumar MV, Hessini K, Subramaniyam S, Sivaramakrishnan R, Kanniappan GV, Jayaraman S, Palanisamy CP. Green fabrication of starch/PVA/CuO nanoscaffolds using marine macroalgae extract for enhanced anti-inflammatory activity. Sustainable Chemistry and Pharmacy. 2026; 51: 102397.
[25] Balasubramanian V, Loganathan L, Muthuswamy K, Viswanathan TM, Raju MV, Chandrasekaran MK, Ahalliya RM, Poorasamy J, Palanisamy CP, Dominic S, Kanniappan GV. Anticancer therapeutic efficacy of PEGylated β-galactosidase from Aspergillus terreus in DMBA-induced breast cancer: Toxicological, molecular and histopathological evaluation in Wistar rats. International Journal of Biological Macromolecules. 2026; 360: 151856.
[26] Jayaraman S, Eswaran A, Rajagopal P, Palanisamy CP, Veerakumar P, Veeraraghavan VP, Sirasanagandla SR. Neuroendocrine-associated epigenetic factors in cellular senescence: mechanisms and therapeutic implications. Biogerontology. 2026; 27(2): 64.
[27] Ponnusamy B, Rajagopal P, Palanisamy CP, Veeraraghavan VP, Jayaraman S. Mechanistic Exploration of the anticancer activity of Justicia adhatoda Plant Leaf Ethanolic Extract against Colon Cancer Cells: An in silico and in vitro Approach. Asian Pacific Journal of Cancer Prevention. 2026; 27(3): 1069-1080.
[28] Pei J, Saran VS, Sivaramakrishnan R, Kanniappan GV, Pandurangan V, Jayaraman S, Dhayalan VK, Mironescu M, Mironescu ID, Palanisamy CP. Ultrasonic-assisted, Sargassum ilicifolium (brown marine macroalgae)-mediated biogenic synthesis of CuO nanoparticles incorporated in starch/PVA electrospun nanoscaffolds: In vitro safety and antioxidant efficacy assessment. Bioorganic Chemistry. 2026; 173: 109679.
[29] Raj MAPA, Subramaniyam S, Kanniappan GV, Jayaraman S, Palanisamy CP. Sustainable fabrication of starch/PVA/CuO electrospun nanoscaffolds from Turbinaria ornata (marine macroalgae) extract: Physicochemical characterization and antidiabetic evaluation. Kuwait Journal of Science. 2026; 53(2): 100545.
[30] Pei J, Ganesh NS, Subramaniyam S, Sivaramakrishnan R, Kanniappan GV, Jayaraman S, Palanisamy CP. Sustainable fabrication of starch/PVA/CuO electrospun nanoscaffolds from Padina tetrastromatica (Brown macroalgae) extract: Physicochemical characterization and antidiabetic assessment. Sustainable Chemistry One World. 2026; 9: 100195.
[31] Sakthiraj A, Sivaramakrishnan R, Subramaniyam S, Kanniappan GV, Pandurangan V, Jayaraman S, Dhayalan VK, Mironescu M, Mironescu ID, Palanisamy CP. Starch/PVA electrospun nanoscaffolds loaded with ultrasonic-assisted green-synthesis of CuO nanoparticles from marine macroalgae (Gracilaria corticata) extract: Cytotoxicity and antioxidant analysis. Chemical Physics Impact. 2026; 12: 101018.
[32] Raju M, Chandrasekaran MK, Loganathan L, Ahalliya RM, Mironescu M, Mironescu ID, Palanisamy CP, Kanniappan GV. Lipid remodeling and ferroptosis in phosphatidylcholine-mediated tumor–stroma crosstalk. Frontiers in Molecular Biosciences. 2026; 13: 1742305.

[33] Kunamalla R, Panagal M, Palanisamy CP. Biogenic synthesis and fabrication of starch/PVA/CuO electrospun nanoscaffolds from Sargassum ilicifolium (brown marine macroalgae) extract for anticancer activity on HT-29 and MCF-7 cancer cells. Biocatalysis and Agricultural Biotechnology. 2026; 72: 103923.
[34] Pei J, Govindaraj H, Sivaramakrishnan R, Kanniappan GV, Pandurangan V, Dhayalan VK, Mironescu M, Mironescu ID, Jayaraman S, Palanisamy PC. Sustainable fabrication of biopolymer-based (starch/PVA) nanoscaffolds loaded with green-synthesized CuO nanoparticles from Sargassum wightii (marine macroalgae): Cytocompatibility and antioxidant activity. Biomaterials Advances. 2026; 182: 214660.
[35] Pei J, Perumal NC, Meng P, Long Q, Palanisamy CP. Extracellular vesicle-based biosensors for Alzheimer's disease: A new frontier in precision diagnostics. Ageing Research Reviews. 2026; 113: 102904.
[36] Shree P, Sivaramakrishnan R, Kanniappan GV, Pandurangan V, Jayaraman S, Dhayalan VK, Mironescu M, Mironescu ID, Palanisamy CP. Antioxidant and biocompatible CuO-starch/PVA nanoscaffolds via ultrasonic green synthesis using Turbinaria conoides (brown marine macroalgae). Medicine in Drug Discovery. 2025; 28: 100238.
[37] Gong J, Lin J, Guan T, Pei J, Palanisamy CP, El-AtyFrom AMA. selenium tolerance to nanoplastic antagonism: Comprehensive characterization of L. casei SNUT1 and its extracellular vesicle–nanoselenium complex. Food Bioscience. 2025; 74: 107749.
[38] Poochi SP, Sundarraj R, Raju MV, Chandrasekaran MK, Ahalliya RM, Palanisamy CP, Kanniappan GV, Kondapavuluri BK, Thiruvengadam M. Harnessing Nature: Computational and Experimental Insights Into *Ipomoea obscura* Metabolites for Bladder Cancer Therapy. Chemistry and Biodiversity. 2025; 0: e00909.
[39] Dugganaboyana GK, Kannankumar MKG, Shivaramakrishna S, Raju MV, Chandrasekaran MK, Ahalliya RM, Panneerselvam N, Palanisamy CP, Kanniappan GV. Phytochemical insights, antioxidant activity and therapeutic potential of Cassia senna against prostate cancer in Wistar albino rats. Discover Applied Sciences. 2025; 7:1206.
[40] Natarajan SR, Krishnamoorthy R, Alshuniaber MA, Gatasheh MK, Rajagopal P, Veeraraghavan VP, Palanisamy CP, Jayaraman S. KDM1A Facilitates Oncogenic Potential in Colorectal Cancer Progression Through the Activation of AXIN/GSK3β/β-Catenin Signaling Pathways: Evidence From Integrated Transcriptomics and In Vitro Studies. The Journal of Gene Medicine. 2025; 27(11): e70053.
[41] Guan T, Gong J, Lin J, Palanisamy CP, Jinjin Pei J, El-Aty AMA. Machine learning-driven multimodal optimization of selenium biotransformation and flavor profiling in fermented apple–Yacon functional beverages. Innovative Food Science & Emerging Technologies. 2025; 105: 104198.
[42] Natarajan SR, Krishnamoorthy R, Alshuniaber MA, Alsulami TS, Gatasheh MK, Rajagopal P, Palanisamy CP, Govindan R, Veeraraghavan VP, Jayaraman S. ABCE1 facilitates tumour progression via aerobic glycolysis and inhibits cell death in human colorectal cancer cells through the p53 signalling pathway. Scientific Reports. 2025; 15: 24674.
[43] Huang Y, Guo H, Liu Y, Jin W, Palanisamy CP, Pei J, Oz F, El-Aty AMA. Effects of Natural Polysaccharides on the Gut Microbiota Related to Human Metabolic Health. Molecular Nutrition & Food Research. 2025; 69:e202400792.
[44] Poornima K, Meenakshi K.C, Manikandan V.R, Shankari G, Prabhu D, Rathi M.A, Palanisamy CP, Balaji R, Gopalakrishnan V.K. Exploring the anticancer potential of Jerantinine A from *Tabernaemontana coronaria* against prostate, breast, and ovarian cancers: A computational approach. *Journal of Complementary and Integrative Medicine*, 2025 22(2): 363–372.
[45] Palanisamy CP, Poompradub S, Sansanaphongpricha K, Jayaraman S, Subramani K. Faridah Sonsudin gGreen synthesis of Nigella sativa-mediated silver nanoparticles for enhanced antibacterial activity and wound healing: Mechanistic insights and biomedical applications. Environmental Nanotechnology, Monitoring & Management. 2025; 24: 101085.
[46] Surendran N, Raju MV, Chandrasekaran MK, Ahalliya RM, Palanisamy CP, Chandrasekaran G, Kanniappan GV. Physicochemical characterization of starch from Maranta arundinacea L.(arrowroot) rhizomes and its inhibition of COX-2: In vivo validation. Bioactive Carbohydrates and Dietary Fibre. 2025; 33: 100465.
[47] Kannappan P, Chandrasekaran MK, Raju MV, Gopalakrishnan S, Dhamodharan P, Ahalliya RM, Palanisamy CP, Raju B, Kanniappan GV. Exploring the anticancer potential of Jerantinine A from Tabernaemontana coronaria against prostate, breast, and ovarian cancers: a computational approach. Journal of Complementary and Integrative Medicine. 2025; 22(02): 363-372.
[48] Pei J, Kumarasamy RV, Jayaraman S, Kanniappan GV, Long Q, Palanisamy CP. Quercetin-functionalized nanomaterials: Innovative therapeutic avenues for Alzheimer's disease management. Ageing Research Reviews. 2025; 104: 102665.
[49] Jayaraman S, Prasad M, Natarajan SR, Krishnamoorthy R, Alshuniaber MA, Gatasheh MK, Veeraraghavan VP, Rajagopal P, Palanisamy CP. Molecular mechanisms underlying the effects of beta-sitosterol on TGF-β1/Nrf2/SIRT1/p53-mediated signaling in the kidney of a high-fat diet and sucrose-induced type-2 diabetic rat. Chemico-Biological Interactions. 2025; 411: 111443.

[50] Huang Y, Guo H, Liu Y, Jin W, Palanisamy CP, Pei J, Oz F, El-Aty AMA. Effects of Natural Polysaccharides on the Gut Microbiota Related to Human Metabolic Health. Molecular Nutrition & Food Research. 2025; e202400792.
[51] Prabhakaran P, Palanisamy CP, Shanmugam A, Damodharan P, Swaminathan H, Devaraj D, Ahalliya RM, Kanniappan GV. Isolation, structural characterization, and molecular docking studies on the bioactive compound from n-Hexane extract of Emilia sonchifolia (L.) DC against the pancreatic cancer target Aurora 2 Kinase. Journal of Complementary and Integrative Medicine. 2024; 22(1): 0290.
[52] Jiang H, Kumarasamy RV, Pei J, Raju K, Kanniappan GV, Palanisamy CP. Integrating engineered nanomaterials with extracellular vesicles: Advancing targeted drug delivery and biomedical applications. Frontiers in Nanotechnology. 2024; 6: 1513683.
[53] Guo H, Liu Y, Wan T, Song D, Palanisamy CP, Geng J, Pei J, Özmen S, El-Aty AMA. Toward personalized cancer management: Role of precision nutrition–diet interventions. Journal of Functional Foods. 2024; 123: 106584.
[54] Natarajan SR, Krishnamoorthy R, Alshuniaber MA, Al-Anazi KM, Farah MA, Rajagopal P, Palanisamy CP, Veeraraghavan VP, Jayaraman S. Identification of FOXM1 as a novel protein biomarker and therapeutic target for colorectal cancer progression: Evidence from immune infiltration and bioinformatic analyses. International Journal of Biological Macromolecules. 282 (Part 4): 137201.
[55] Rajendran MS, Jayaraman S, Khan JM, Jasmine S, Prabhakaran RK, Raju MV, Chandrasekaran MK, Ahalliya RM, Kannappan P, Palanisamy CP, Kanniappan GV. Investigating the colon toxicity and carcinogenic role of monosodium glutamate compared with Dimethylhydrazine in male Wistar rats: Exploring the link to childhood colon cancer risk. Journal of King Saud University - Science. 2024; 36(11): 103507.
[56] Kumarasamy RV, Natarajan P, Umapathy VR, Roy JR, Rab SO, Saeed M, Panagal M, Mironescu M, Srinivasan GP, Palanisamy CP. Clinical Applications and Therapeutic Potentials of Advanced Nanoparticles: A Comprehensive Review on Completed Human Clinical Trials. Frontiers in Nanotechnology. 2024; 6:1479993.
[57] Jin W, Pei JJ, Roy JR, Jayaraman S, Ahalliya RM, Kanniappan GV, Mironescu M, Palanisamy CP. Comprehensive review on single-cell RNA sequencing: A new frontier in Alzheimer's disease research. Ageing Research Reviews. 2024; 274: 102454.
[58] Pei J, Palanisamy CP, Jayaraman S, Natarajan PM, Umapathy VR, Roy JR, Panagal M, Jayaraman S. Curcumin-loaded polymeric nanomaterials as a novel therapeutic strategy for Alzheimer's disease: A comprehensive review. Ageing Research Reviews. 2024; 99: 102393.
[59] Pei J, Palanisamy CP, Jayaraman S, Natarajan PM, Umapathy VR, Roy JR, Thalamati D, Ahalliya RM, Kanniappan GV, Mironescu M. A comprehensive review on starch-based Sustainable Edible Films Loaded with Bioactive Components for Food Packaging. International Journal of Biological macromolecules. 2024; 274 (Part-1): 133332.
[60] Palanisamy CP, poompradub S, Sansanaphongpricha K, Subramani K, Sonsudin F. Increased expression levels of PDGF and VEGF magnify the wound healing potential facilitated by biogenic synthesis of silver nanoparticles. Nano-Structures & Nano-Objects. 2024; 39: 101236.
[61] Pei J, Palanisamy CP, Jayaraman S, Natarajan PM, Umapathy VR, Roy JR, Thalamati D, Ahalliya RM, Kanniappan GV, Mironescu M. Proteomics Profiling of Extracellular Vesicle for Identification of Potential Biomarkers in Alzheimer's Disease: A Comprehensive Review. Ageing Research Reviews. 2024; 99: 102359.
[62] Xi J, Wang T, Xian P, Liu X, Du M, Yang H, Palanisamy CP, Lin W, Long Q. Proteomic insights uncover enhanced neurotherapeutic potential in conditioned mesenchymal stem cell-derived extracellular vesicles. Extracellular Vesicle. 2024; 3: 100037.
[63] Pei J, Natarajan PM, Umapathy VR, Swamikannu B, Sivaraman NM, Krishnasamy L, Palanisamy CP. Advancements in the synthesis and functionalization of zinc oxide-based nanomaterials for enhanced oral cancer therapy. Molecules. 2024; 29(11): 2706.
[64] Gatasheh MK, Natarajan SR, Krishnamoorthy R, Alsulami TS, Rajagopal P, Palanisamy CP, Veeraraghavan VP, Jayaraman S. Molecular analysis to identify novel potential biomarkers as drug targets in colorectal cancer therapy: an integrated bioinformatics analysis. Molecular and Cellular Oncology. 2024; 11(1): 2326699.
[65] Pei J, Yan Y, Jayaraman S, Rajagopal P, Natarajan PM, Umapathy VR, Gopathy S, Roy JR, Sadagopan CS, Thalamati D, Palanisamy CP, Mironescu M. A review on advancements in the application of starch-based nanomaterials in biomedicine: Precision drug delivery and cancer therapy. International Journal of Biological Macromolecules. 2024; 130746.
[66] Pei JJ, Yan Y, Palanisamy CP, Jayaraman S, Natarajan PM, Umapathy VR, Gopathy S, Roy JR, Sadagopan JC, Thalamati D, Mironescu M. Materials-based drug delivery approaches: Recent advances and future perspectives. Green Processing and Synthesis. 2024; 13: 20230094.

[67] Pei JJ, Deng W, Liu Y, Guo Y, Chen J, Abdu H, Khan MR, Palanisamy CP, El-Aty AM. A Comprehensive Review of Cornus officinalis: Health Benefits, Phytochemistry, and Pharmacological Effects for Functional Drug and Food Development. Frontiers in Nutrition. 2023; 10: 1309963.
[68] Alugoju P, Palanisamy CP, Anthikapalli NVA, Jayaraman S, Prasanskulab A, Chuchawankul S, Dyavaiah M, Tencomnao T. Exploring the anti-aging potential of natural products and plant extracts in budding yeast Saccharomyces cerevisiae: A review. F1000Research. 2023; 12: 1265.
[69] Lavanya M, Krishnamoorthy R, Alshuniaber MA, Manoharadas S, Palanisamy CP, Veeraraghavan VP, Jayaraman S, Rajagopal P, Padmini R. Formulation, characterization and evaluation of gelatin-syringic acid/zinc oxide nanocomposite for its effective anticancer, antioxidant and anti-inflammatory activities. Journal of King Saud University-Science. 2023; 35: 102909.
[70] Palanisamy CP, Poompradub S, Sansanaphongpricha K, Jayaraman S, Subramani K, Sonsudin F. Biosynthesis of silver nanoparticles (AgNPs) using ethanolic extract of Nigella sativa (L.) seeds promotes wound healing via PDGF and VEGF signalling pathways activation. Biocatalysis and Agricultural Biotechnology. 2023; 54: 102970.